processes

MDPI

Article

Design and Characterization of a Continuous Melt Milling Process Tailoring Submicron Drug Particles

Philip da Igreja [1,2], Tim Grenda [2], Jens Bartsch [2] and Markus Thommes [2,*]

[1] INVITE GmbH, Chempark Building W32, 51368 Leverkusen, Germany; philip.daigreja@tu-dortmund.de
[2] Laboratory of Solids Process Engineering, Department of Biochemical and Chemical Engineering, TU Dortmund University, 44227 Dortmund, Germany
* Correspondence: professors.fsv.bci@tu-dortmund.de; Tel.: +49-231-755-6088

Abstract: Solid crystalline suspensions (SCSs) containing submicron particles were introduced as a competitive solution to increase dissolution rates and the bioavailability of poorly water-soluble drugs. In an SCS, poorly water-soluble drug crystals are finely dispersed in a hydrophilic matrix. Lately, melt milling as an adapted wet milling process at elevated temperatures has been introduced as a suitable batch manufacturing process for such a formulation. In this work, the transfer from batch operation to a two-step continuous process is demonstrated to highlight the potential of this technology as an alternative to other dissolution-enhancing methods. In the first step, a powder mixture of a model drug (griseofulvin) and a carrier (xylitol) is fed to an extruder, where a uniform suspension is obtained. In the second step, the suspension is transferred to a custom-built annular gap mill, where comminution down to the submicron region takes place. The prototype's design was based on batch grinding results and a narrow residence time distribution, intended to deliver large quantities of submicron particles in the SCS. The throughput of the mill was found to be limited by grinding media compression. By inclining the mill at an angle, the grinding media position was manipulated, such that compression was avoided. Different states of the grinding media in the grinding chamber were identified under surrogate conditions. This strategy allows the maintenance of an energy-optimized comminution without adaption of the associated process parameters, even at high throughputs. Using this new process, the production of an SCS with 80–90 % submicron particles in a single passthrough was demonstrated.

Keywords: solid crystalline suspension; submicron particles; comminution; prototype; pharmaceutical application; continuous process

check for updates

Citation: da Igreja, P.; Grenda, T.; Bartsch, J.; Thommes, M. Design and Characterization of a Continuous Melt Milling Process Tailoring Submicron Drug Particles. *Processes* **2024**, *12*, 1417. https://doi.org/10.3390/pr12071417

Academic Editor: Evangelos Tsotsas

Received: 12 June 2024
Revised: 29 June 2024
Accepted: 3 July 2024
Published: 7 July 2024

Copyright: © 2024 by the authors. Licensee MDPI, Basel, Switzerland. This article is an open access article distributed under the terms and conditions of the Creative Commons Attribution (CC BY) license (https://creativecommons.org/licenses/by/4.0/).

1. Introduction

Melt milling, an adaptation of the wet milling process, currently focuses on the pharmaceutical sector and aims to address one of the industry's key issues. Over the years, the structures of active pharmaceutical ingredients (APIs) have become increasingly more complex. This leads to a limited aqueous solubility and slow dissolution rates for most of these new chemical entities. Here, particle size reduction was found to be a universal tool to enhance the dissolution performance of such APIs (class II according to the biopharmaceutical classification system [1]). In this context, wet milling, for example carried out in a stirred media mill, is an effective top-down approach to reliably achieve submicron (0.1–1 µm) or nanoparticle (<0.1 µm) suspensions with high drugs loads. Compared to common bottom-up approaches, such as precipitation or spray-drying, which use organic solvents to dissolve the API before processing, wet milling usually relies on water, making it also the eco-friendlier alternative [2]. However, wet grinding has a major disadvantage in that Ostwald ripening and agglomeration processes render the resulting suspension unstable. Therefore, the liquid phase must be subsequently removed to obtain a re-dispersible solid.

This challenge can be circumvented by formulating the poorly water-soluble API as a solid crystalline suspension (SCS) [3–6]. In this subtype of solid dispersions, the finely

ground crystalline particles are contained in a crystalline, hydrophilic carrier matrix, which acts as the continuous phase. In melt milling, the carrier matrix is first liquified at elevated temperatures and the API selectively ground below its own melting point. After removal of the grinding media, the partially molten suspension is quench-cooled and the ground particles are immobilized upon solidification, resulting in a long-term stable product. Upon introduction of the SCS to an aqueous media, the carrier is dissolved and the particles are released in their ground state.

In a first study, the production of an SCS via melt milling with submicron contents of >90% and improved dissolution performance was demonstrated, using a custom-built annular gap mill. Melt milling was found to not affect the solid-state properties of the griseofulvin–xylitol system. In a second study, the incorporation of a gas phase (air) into the melt led to an improved release of primary particles from the matrix. In a comparison, the foamed SCS outperformed an unformulated SCS, likely due to the larger surface area of dispersed primary particles compared to predominantly agglomerates in the second case [7,8].

Thus far, melt milling has been carried out as a batch process. In contrast, the research focus and interest of the pharmaceutical industry have shifted towards continuous manufacturing within the last decade to benefit from a consistent product quality during steady-state operation, lower cycle times and manufacturing costs [9–11]. Thus far, continuous wet grinding of submicron- or nanosized drug particles is not commonly applied, as long grinding times (up to several hours [12]) can be required for a sufficient fineness. In theory, the targeted quality could be achieved by using a cascade of 5–12 mills [13,14]. Yet, this approach is often not feasible for research purposes due to the enhanced costs. Patented top-down or combinatory technologies, such as NanoCrystal™ [15,16], DissoCubes® [17,18], NanoPure®, NANOEDGE™ [19] only operate in recirculation, pendulum, or multi-passage modes to achieve a continuous-like state. In summary, and with respect to the literature, a truly continuous, economical technology for the execution of melt milling is missing to date.

Consequently, in this work the design, implementation, and evaluation of a two-step process concept for continuous melt milling is presented. It combines gravimetric feeding, extrusion, and comminution for the production of an SCS. In this process, a mill is applied, which was specifically designed to provide sufficient residence time for a high submicron content in a single passage. Batch grinding experiments were conducted on pre-extruded material to model the particle size distribution (PSD) of the SCS, using different mill designs. The physical prototype is characterized in terms of residence time distribution (RTD) as a key process parameter to obtain process boundaries. As the chosen design promotes grinding media compression, process limits regarding the maximum throughput were identified. A tilting strategy to shift these throughput limits was implemented. The impact of this tilting strategy on the RTD was evaluated. Finally, an SCS was produced using a previously described setup, to evaluate the overall process performance and uncover potential improvements.

2. Materials and Methods

2.1. Materials

Micronized griseofulvin (Hawkins, Minneapolis, MN, USA), with a melting point of 220 °C, was employed as a poorly water-soluble model drug. Xylitol (Xylisorb 300, Roquette, Lestrem, France) acted as a hydrophilic carrier matrix and has a melting point of 94 °C. Spherical zirconium dioxide with a diameter of 0.3 mm (Zetabeads Plus, Netzsch Vakumix, Weyhe-Dreye, Germany) served as grinding media. Sodium dodecyl sulfate (SDS) (Fluka, Buchs, Switzerland) was used to stabilize griseofulvin particles during particle size measurements, while sodium chloride (Sigma Aldrich, Burlington, MA, USA) served as a tracer substance for the determination of RTDs.

2.2. Methods

2.2.1. Particle Size Determination

Particle size distributions were measured by laser diffraction (Mastersizer 3000, Malvern Instruments, Malvern, UK). A wet dispersion unit (Hydro EV) was used to disperse the SCS in a filtered, saturated drug solution assisted by agitation via stirring (2500 1/min) and ultrasound. Upon dissolution of the surrounding xylitol matrix in the dispersant, the released griseofulvin particles could be analyzed. Measurements were carried out under permanent agitation until agglomerates were fully broken up. Reagglomeration of primary drug particles was inhibited by adding 3 mL 2.5 w.% SDS solution from the start. Only the particle size of these primary particles is reported within this work. Additional details and material parameters can be found in a related publication [7].

2.2.2. Batch Grinding

The grinding kinetic of the pre-extruded SCS (compare Section 2.2.3) was determined in a custom-built annular gap batch mill. Samples were taken based on elapsed grinding time and covered a total of 90 min. Sampling intervals were densified to 2.5 min for the first 20 min, as particle size changes significantly in the early phase of grinding. Afterwards, samples were taken at the 30 and 90 min marks of the total process time. Based on previous investigations, the drug load was 10 w.%, the rotor tip speed was 12 m/s, and the filling ratio with 0.3 mm zirconium dioxide grinding media was 80%. For detailed information about the setup and procedure, refer to da Igreja et al. [7].

2.2.3. Continuous Manufacturing

Within this work, the continuous manufacturing of an SCS is demonstrated in a single passage carried out as the following two-step process: First, a griseofulvin–xylitol powder mixture with 10 w.% drug load is continuously fed by a gravimetric solid feeder (K-ML-SFS-KT20, Coperion K-Tron, Niederlenz, Switzerland) to a co-rotating twin-screw extruder (ZSE 27 Maxx, Leistritz, Nuremberg, Germany), which melts only the matrix material, so that distributive mixing leads to a uniform suspension. Second, the suspension is continuously fed to a heated annular gap mill prototype, which offers grinding capabilities to the submicron region. A stirred low-volume glass vessel between extruder and mill acts as a buffer tank. The process flow diagram of the continuous manufacturing setup is given in Figure 1.

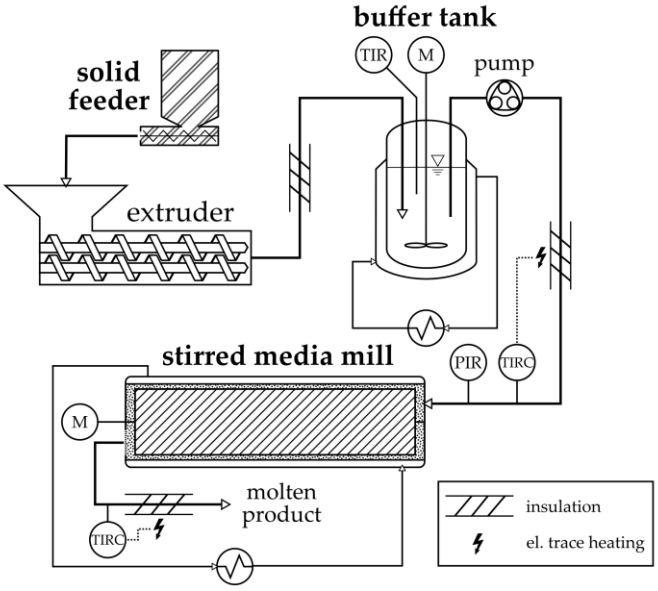


Figure 1. Process flow diagram for the continuous production of solid crystalline suspensions.

During start up, the inclined mill was filled with glycerol against the intended flow direction (outlet to inlet) to remove residual air. Glycerol at 120 °C was fed from the buffer tank using a peristaltic pump (RZR 2, Heidolph Instruments, Schwabach, Germany) with temperature-resistant tubing (Pharmed® BPT, Saint-Gobain, Courbevoie, France) for pre-heating of the equipment. This setup was also used to pump the molten suspension to the mill. The stirred buffer tank and the mill were each heated by separate thermostats (F25 HE and FP50 HL, Julabo, Seelbach, Germany). Piping was equipped with temperature-controlled electrical trace heating (KM-HT-201, SAF Wärmetechnik, Mörlenbach, Germany), while ceramic fiber tape insulation was used to minimize heat loss and prevent crystallization. During the pre-heating phase, the motor of the mill was switched off to avoid blockage.

When temperature levels across the inlet and outlet were constant, the intermeshing twin-screw extruder was fed with the powder mixture via its hopper. Screw speed was set to 250 1/min. The screw configuration shown in Figure 2 was derived from the work of Reitz [5] and consists of pressure build-up zones in front of a main kneading section and the die. The barrel temperature profile is given alongside, and was tailored to allow the suspension to exit with a defined excess temperature into the unheated pipe. The extruder setup was also used to obtain the pre-extruded SCS for the determination of the batch grinding kinetics (see Section 2.2.2).

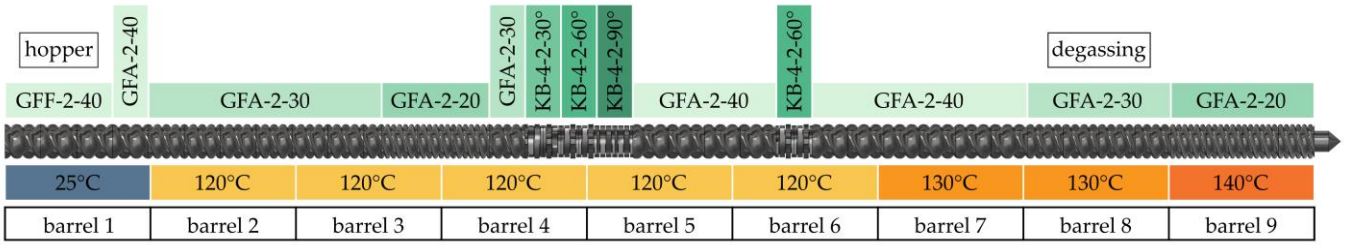


Figure 2. Screw configuration and barrel temperature profile of the extruder used in continuous grinding experiments. Naming scheme: conveying element (GFF/GFA)—number of flights—pitch (in mm); kneading element (KB)—number of discs—number of flights—rotational disc offset.

2.2.4. Residence Time Distribution

The residence time of the annular gap mill was determined via a step response experiment. For this, the conductivity of an aqueous sodium chloride tracer solution was measured in 0.2 Hz intervals at the outlet using an in-line probe (Multi 3410/TetraCon 925, Xylem Analytics, Weilheim, Germany). The solution was pumped at 870 g/h by a mass flow-controlled pump (custom-built). Parameters of the distributions were derived by fitting the closed–closed solution of the axial dispersion model according to Stehr [20] to the experimental data.

3. Results

3.1. Mill Design

The objective was to design a continuously operating process that can achieve a high submicron particle content in a single passage of the material, with the prototype annular gap mill as the main comminution equipment. Therefore, the relevant process parameters and their ranges must be considered during the design phase. The groundwork for this was established in a previous work on the melt milling of the griseofulvin-xylitol system [7]. Using different stress intensities and frequencies in a custom annular gap batch mill, the energy utilization was optimized for a rapid comminution towards the submicron particle size. The obtained values are summarized in Table 1 and served as the basis for the continuous process design phase.

Table 1. Energy-optimized parameter set for melt milling griseofulvin in xylitol [7].

Process Parameters	rotor tip speed v_{tip}	12 m/s
	filling ratio φ_{GM}	80%
	annular gap width	4 mm
Grinding Media Properties	shape	spherical
	diameter d_{GM}	300 µm
	material	yttrium-stabilized zirconium oxide
	density	6000 kg/m^3

A mathematical model was used to gain insight into the influence of different design choices regarding hold-up volume and flow patterns on the resulting particle fineness. The cumulative PSD $Q_3(d_P)_{\bar{t}}$ obtained from continuous melt milling, for a certain particle size d_P and a median residence time $\bar{t}$, can be predicted from a batch grinding kinetic $Q_{3,batch}(t, d_p)$ and an assumed RTD density function $E(t)_{\bar{t}}$ according to Equation (1) [20].

$$Q_3(d_p)_{\bar{t}} = \int_0^\infty Q_{3,batch}(t, d_p) \cdot E(t)_{\bar{t}} dt \quad (1)$$

The resulting prediction of the PSD is only valid if identical stress conditions are applied for the continuous and the batch case. Therefore, the mill geometry and its key dimension had to be maintained, as changes to the rotor/stator proportions could alter the energy transfer. The annular gap design was carried over as it provides a narrow RTD [21,22], which is considered favorable with regard to a uniform PSD.

The first step was to conduct a batch grinding experiment using the energy-optimized process parameters (also see Section 2.2.2 and Table 1) to obtain $Q_{3,batch}(t, d_p)$ for the fastest observed comminution. A deviation towards non-optimized process parameters would have prolonged the grinding times, making continuous manufacturing impossible. Next, the time-discrete particle size data, representing the batch grinding kinetic, were fitted to the first order solution of the population balance model in Equation (2) [23]. This smooths the results of Equation (1). It does so by enabling the numerical integration at any step size, rather than being bound to the sampling intervals of the batch grinding experiment.

$$Q_{3,batch}(t, d_p) = 1 - R(t, d_p) = 1 - \left(y_0 + R(t = 0, d_p) \cdot e^{-S(d_p) \cdot t}\right) \quad (2)$$

The cumulative oversize function $R(t, d_p)$ describes the fraction larger than a given particle size d_p at a certain timepoint t. The selectivity parameter $S(d_p)$ and the offset y_0 were used as independent variables, while $R(t = 0, d_p)$ was constrained by the PSD of the raw material. A total of 101 particle size classes d_p, based on the default output of the laser diffraction system, were fitted.

The axial dispersion model was chosen to represent the residence time distribution $E(t)$, as it is applicable to annular gap mills and can be parameterized only by its mean transportation velocity ($\bar{u}_{ax} = L_{GC}/\bar{t}$) and the Peclet number (Pe) [21]. Various solutions to Equation (1) were generated using variations for $E(t)$. Solutions for $Pe \leq 16$, which represents a back-mixed system, were calculated from the closed–closed solution in Equation (3), according to Mavros [24].

$$E(\theta) = \exp\left(\frac{Pe}{2} \cdot \left(1 - \frac{\theta}{2}\right)\right) \cdot \sum_{n=1}^{\infty} \frac{\lambda_n \cdot (Pe \sin(\lambda_n) + 2\lambda_n \cos(\lambda_n))}{\lambda_n^2 + \frac{Pe^2}{4} + Pe} \cdot \exp\left(-\frac{\lambda_n^2}{Pe}\theta\right)$$
$$\text{with } \tan(\lambda_n) = \frac{4\lambda_n Pe}{4\lambda_n^2 - Pe^2} \text{ and } \theta = \frac{t}{\bar{t}} \quad (3)$$

For Pe > 16, the analytical open–open solution (Equation (4)) was used as an approximation of a system close to a plug-flow characteristic [24].

$$E(\theta) = \sqrt{\frac{Pe}{4\pi\theta^3}} \cdot \exp\left(-\frac{Pe(1-\theta)^2}{4\theta}\right) \quad (4)$$

For a single passage of the material, the mean residence time $\bar{t}$ is approximately equal to the ideal filling time t_f, which can be connected to the grinding chamber volume V_{GC} and operating conditions, such as grinding media volume V_{GM} and volume flow rate $\dot{V}_{susp}$ [21]

$$\bar{t} \approx t_f = \frac{V_{GC} - V_{GM}}{\dot{V}_{susp}} \quad (5)$$

Based on the combination of Equations (2)–(5) with (1), the submicron content $Q_3(d_P = 1\ \mu m)$, which acts as the key quality attribute of an SCS, can be predicted as a function of time and the material transport pattern (Figure 3).

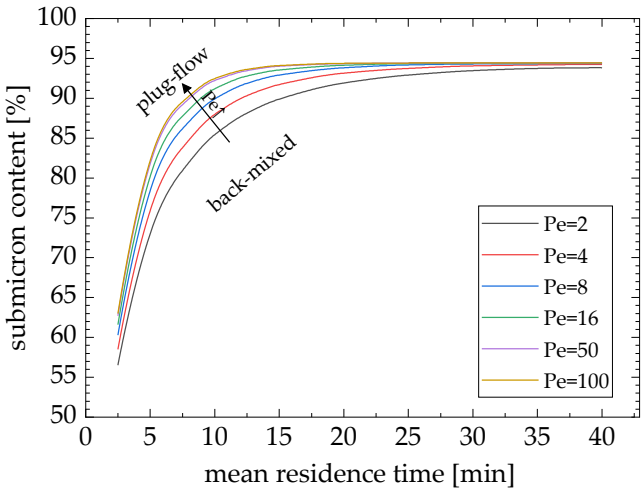


Figure 3. Predicted submicron content $Q_3(d_P = 1\ \mu m)$ in case of continuous melt milling as a function of mean residence time and Peclet number (Pe).

An increase in the mean residence times leads to a shift in the submicron content up to a value of ~94%, regardless of Pe number. At this point, an insufficient colloidal stability suppresses comminution (grinding limit), which matches the behavior of the underlying physical system. With a shift from back-mixed to plug-flow behavior (Pe↑), the required mean grinding time for a constant submicron content will decrease. The reduced short-circuit flow, associated with the plug-flow, lowers the coarse fraction in the product.

Although a mean axial transport velocity $\bar{u}_{ax}$ can be assumed based on the throughput and length of the mill L_{GC}, the Pe number ($Pe = \bar{u}_{ax} \cdot L_{GC}/D_{ax}$) for a certain mill design cannot be determined a priori, because the axial dispersion coefficient D_{ax} is unknown. A complex fluid dynamic model describing all interactions between fluid and solid phases would be required for this. However, according to Figure 3, the influence of axial dispersion on the submicron content is only relevant for short mean residence times, but negligible after 30 min. Hence, this duration was chosen as the target mean residence time in the grinding active zone. The existence of a grinding limit in the unstabilized system does not justify longer grinding times, as it would only lead to additional grinding media wear without improving the product quality.

Figure 4 gives a cross-sectional view of the continuous mill design based on the above-mentioned findings. As the gap width had to be maintained from the batch process in order to not alter stressing conditions and break the validity of Equation (1), achieving the required filling time was only possible by scaling the axial dimension. At a length of 859 mm, corresponding to 30 min of mean residence time, processing of up to 1.27 kg/h SCS can be achieved. Such throughput was considered technically relevant. With a length-to-diameter ratio of 10 (commonly ranging from 1 to 6 [22]), the mill needs to be horizontally started and operated, for the purpose of reducing the (start-up) power draw. Power is provided by a 7.5 kW motor with a frequency converter through a belt–pulley system. The material inside the grinding chamber is 1.4571 stainless steel for the stator and PEEK GF

30 for the rotor. The grinding chamber wall is surrounded by an outer shell to form a jacket for the heat-transfer fluid. In- and outlets for suspension (and heat-transfer fluid) are realized through the flanges, so that the full length of the mill is utilized and a narrower RTD is obtained. Circular screen meshes are integrated into the suspension in- and outlet ports to retain the grinding media. Both ends are equipped with shaft bearings and dual mechanical seals (Cartex DN25, EagleBurgmann, Wolfratshausen, Germany) to stabilize rotary motion. On the outlet-side, the rotor is fixed to the shaft, while on the inlet-side axial movement is allowed to compensate for thermal expansion.

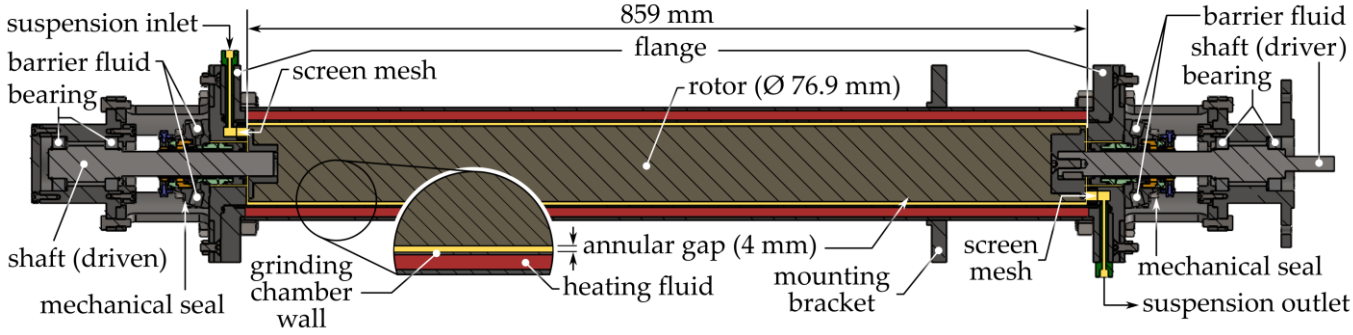


Figure 4. Cut-away view of the continuously operated annular gap mill to produce SCS and a detailed view of the annular gap. The in- and outlet ports for heat-transfer fluid are not visible as they are angled 90° relative to this view.

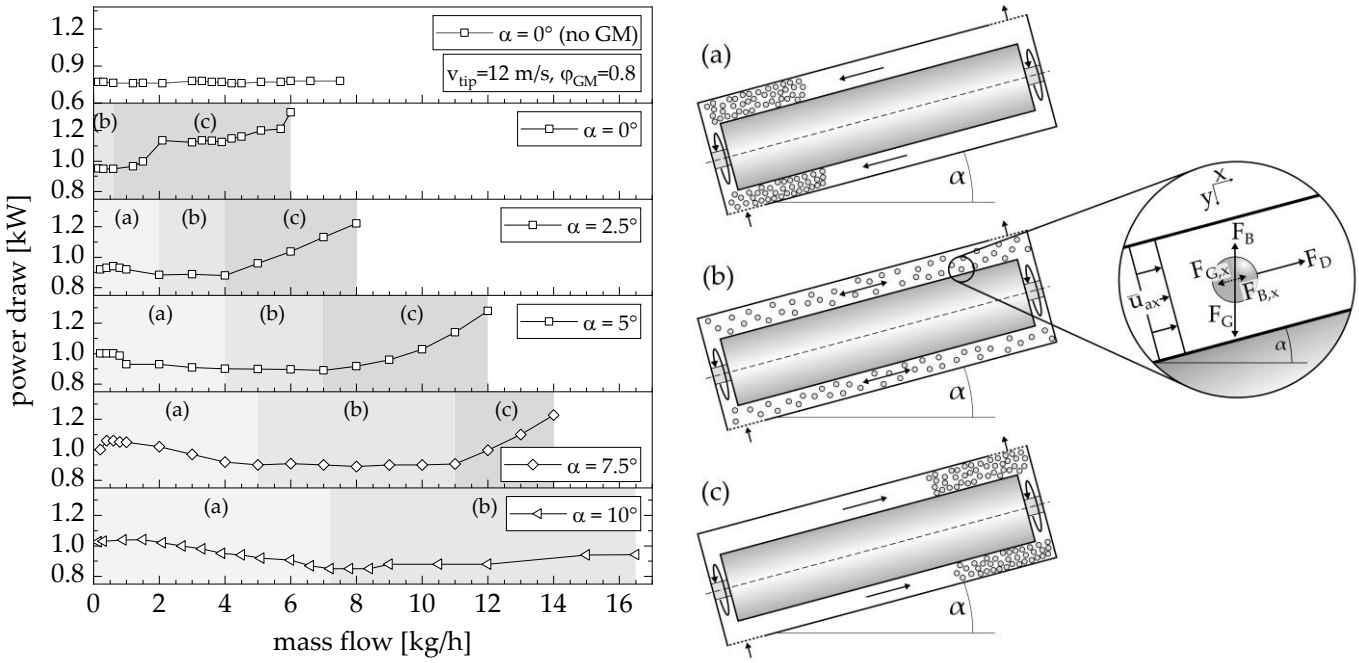
3.2. Design Verification

The initial testing of the mill design focused on the general behavior, the experimentally achievable throughput, and if the set targets could be met. As the applied pressure gradient in continuously operated media mills can introduce grinding media compression, usually at the outlet separation device, a minimum and maximum throughput exist, which define a boundary of the process. Special internal designs can be used to delay the onset of this phenomenon, but the basic annular gap design is prone to blockage because the unobstructed flow path between inlet and outlet does not allow internal bead circulation. Since direct detection of grinding media compression by measuring the local bead distribution (e.g., by radiometric densitometry [25]) is complex, indirect substitute-indicators (motor power and inlet pressure) were employed.

The power draw of the driving motor is given in Figure 5A for different mass flows of water. Without grinding media (GM) and with a horizontal orientation ($\alpha = 0°$) of the mill, the constant power consumption is mainly determined by the friction of the dual mechanical seals (no load power). With grinding media added, bead–bead and bead–wall interactions cause additional friction and the base load increases. After a short initial plateau, the power draw increases for throughputs greater than 0.6 kg/h, which is the typical indication for packing [26]. This operating point is not feasible considering the lower viscosity of water, compared to the more viscous SCS (~200–500 mPas at 120 °C), and the maximum target throughput of up to 1.27 kg/h. A tilt angle α of the mill towards the outlet was applied to introduce sedimentation as a countermeasure for grinding media compression (see forces in Figure 5B). For tilt angles $\alpha > 0°$, three distinct operating regimes can be identified based on the power draw trend. In regime (a), power draw decreases as the throughput increases, regime (b) features a minimum constant power draw, and regime (c) begins when power draw increases rapidly with mass flow. This course can be explained by three distinct states of the grinding media inside the annular gap, visualized in Figure 5B:

(a) Gravitational force ($F_{G,x}$) outweighs drag force (F_D) and buoyancy in axial direction ($F_{B,x}$)—grinding media sediments to the inlet;
(b) Balance of all axial forces—grinding media floats and is evenly distributed;

(c) Drag force (F_D) and buoyancy in axial direction ($F_{B,x}$) outweigh gravitational force ($F_{G,x}$)—grinding media is compressed at the outlet.



(**A**) (**B**)

Figure 5. (**A**) Measured power draw of the mill for different mass flow rates of water and tilt angles α. (**B**) Corresponding regimes' (**a**) bead compression at the inlet, (**b**) uniform distribution, and (**c**) bead compression at the outlet. The detail view (right) shows the relevant forces (B—buoyancy' D—drag; and G—gravitational) and their share in x-direction (direction of flow) acting on a single grinding bead, subjected to a flow velocity $\bar{u}_{ax}$ in the annular gap. The centrifugal force in y-direction is omitted.

For larger tilt angles, onset of the desired regime (b) shifts towards higher mass flow rates, because higher drag force is necessary to counter the growing axial component of the gravitational force acting towards the inlet. A broadening of regime (b) is also observed for a larger α, supposedly due to a self-regulating effect. Beads in a downward motion lower the local porosity at the inlet, increasing the effective flow velocity and thus the drag force, pushing them upward until they are evenly distributed, and the process starts over. For an angle of 10°, the regime (b) extends so far that regime (c) is not observed in the tested throughput range. Usually, packing is strongly connected to the throughput and can only be influenced by an increase in tip speed, bead size, and density or a decrease in filling ratio and viscosity [22]. Adaptions to these key process parameters would decrease energy utilization and come at the cost of a reduced product quality. The tilting approach decouples this relationship, so that optimal process parameters can be applied over a wide range of throughputs without severe packing.

Additionally, glycerol at 20 °C was employed as a substitute liquid, since its density and viscosity closely match that of the molten SCS at 120 °C. The objective was to create comparable forces on the grinding media and identify a stable operating angle α that could be used with the molten suspension. This time, the inlet pressure (Figure 6, top), which is an alternative indirect packing indicator [26], and the outlet mass flow (Figure 6, bottom) were monitored for a set mass flow of 1 kg/h. As the tilt angle of the mill is increased, the equilibrium pressure (pressure after 30 min runtime) steadily decreases to a minimum, which indicates a transition from regime (c) to (b). Similarly, the outlet mass flow increases and matches the set throughput when regime (b) is achieved. Tilting above 12° tips the

force balance and the grinding beads settle at the inlet, causing higher backpressure and lower throughput as the local porosity decreases. In comparison to the determination of the process limits using water, it is confirmed that the usable regime (b) shifts for higher viscosity fluids. The higher drag force on the grinding media requires either lower flow rates at the same angle or larger angles at the same flow. A broad plateau for regime (b) as seen in Figure 5A was not identified in the case of glycerol, which limits the usable operating space. Deviations from the operating point also have a large impact on the system behavior. Yet, these trends still agree with the theoretical considerations of the acting forces given for water. Additionally, product quality was impacted by the specific operating regime. Figure 6 pictures glycerol, processed within regime (c) (3°) and the desired regime (b) (12°). While the former is opaque from abrasion of the metallic grinding chamber, the glycerol processed in regime (b) remains translucent. Therefore, another advantage of the tilting strategy is that wear can be minimized without deviation from the operating parameters with the highest energy utilization.

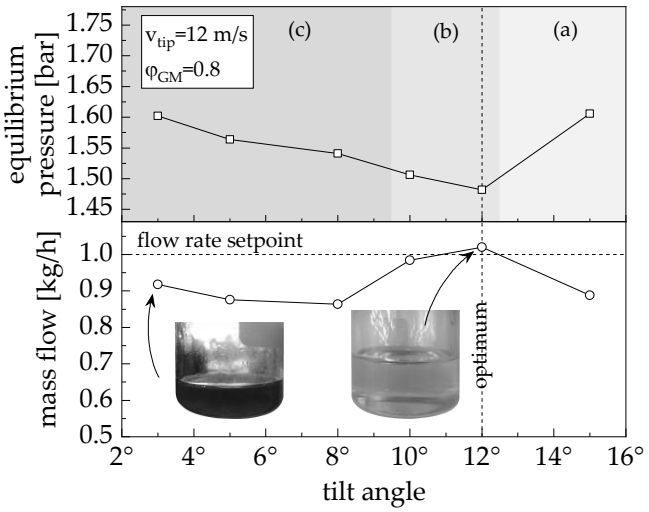


Figure 6. Inlet equilibrium pressure (**top**) and outlet mass flow rate (**bottom**) after 30 min of runtime with glycerol at a set flow rate of 1 kg/h. Pictured at the bottom is glycerol obtained from processing in two different regimes. (**a**), (**b**) and (**c**) refer to the regimes introduced in Figure 5B.

3.3. Residence Time Distribution

In order to uncover the effect of tilting the apparatus on the flow inside the grinding chamber, residence time distributions were measured using an aqueous salt tracer solution. The volume flow was matched to the molten suspension during processing. Figure 7 gives the mean residence time and mean Peclet number for different tilt angles of the mill (bottom), as well as observed power draw ranges (top). The ideal filling time (Equation (5)) of the grinding chamber (t_f) and the hydrodynamic residence time of the system ($t_{f,system}$), which additionally includes the free volume of tubes and peripherals, are given as reference. The closed–closed solution of the axial dispersion model was used to fit the experimental data ($R^2 > 0.99$).

For 0° and 4°, the observed mean residence time is greater than the system filling time, which suggests an increased degree of backflow as the apparent system volume is larger. This agrees with the fitted Peclet numbers for these tilt angles, which are lower in comparison to 8°. For this angle, the mean residence time drops below the system filling time. Power draw increased with the tilt angle, so compression at the inlet is likely to occur. Thus, the trend of the mean residence time in Figure 7 can be explained by the formation of a grinding media-free zone towards the outlet, in which back-mixing is reduced and short-circuit flow is promoted.

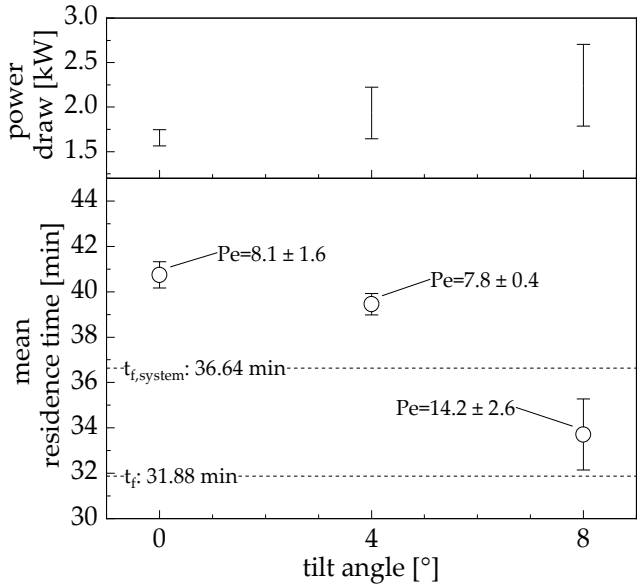


Figure 7. Dependency of the mean residence time (av ± std, n = 3) and Peclet number (av ± std, n = 3) on the tilt angle of the mill. (**bottom**). The dashed lines represent the ideal filling time t_f and $t_{f,system}$ for the grinding chamber and the system including peripherals, respectively. Also given are the observed power draw ranges (**top**).

The measured mean residence times lie within the design scope of Figure 3 and the set target of 30 min. If comminution takes place under packing conditions, deviations in the predicted grinding results are expected, because stressing is not guaranteed over the full length of the mill. Furthermore, higher tilt angles introduced more variability in the mean residence time, which in turn affects the obtained particle size. In consequence, suitable process analytical technology will be implemented to monitor the position and distribution of the grinding media for a pharmaceutical application in future, as non-compliance results in an out-of-specification product based on the above result.

3.4. Process Results

The developed continuous melt milling process involved the extrusion of a powder mixture. In this upstream step, the material is partially melted to form a well-mixed suspension, which is then fed via an intermediary buffer vessel to the mill. During processing, the tilt angle was adapted in response to the measured process parameters. The submicron content and particle size of the final product was evaluated offline from samples taken in regular intervals and is shown in Figure 8, along with the predictions based on the modeling presented in Section 3.1. Only fully recrystallized product was considered to ensure the absence of remaining glycerol. The data start with the washout of glycerol (striped area), which acts as a heat-transfer fluid during startup. After approximately 40 min, the glycerol was washed out based on the samples taken at the outlet, which fully crystallized after the experiment, while previous samples did not. Note that the particle size from the upstream extrusion was constant over the process time and in good agreement with the results during the experiments conducted for the determination of the batch kinetics.

First, the achieved submicron content of 80–90% in the SCS, which was selected as the primary quality attribute, is promising, as it matches the published batch result [7]. Second, the determined sub-micron content is in good agreement with the predictions. This highlights the suitability of the theoretical approach for the design of this mill. Deviations between experiment and prediction likely stem from the fact that stress events did not occur uniformly across the full length of the mill, due to an uneven axial distribution of grinding media (assumption for Equation (1)). More stress events will take place in zones with a high local filling ratio (here, the inlet), while the outlet region of the grinding

chamber contributes less to comminution. Furthermore, the d_{10} and d_{50} were stable across the process time. Inter-sample variability can be explained by the inconsistent mass flow rate, again, causing fluctuations in the number of stress events.

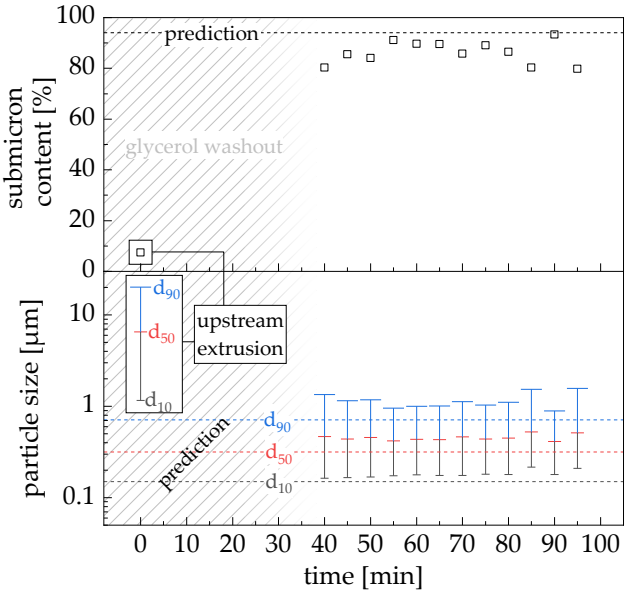


Figure 8. Particle size and submicron content over the process time of a continuous grinding experiment. Predicted values are indicated by horizontal dashed lines, while data points within a box belong to the upstream extrusion. Samples from the glycerol washout phase (striped area) were not considered.

In addition to the product properties, the process characteristics with respect to the power draw, inlet pressure, outlet mass flow (Figure 9), and temperatures at several positions of the mill were also monitored during the tests.

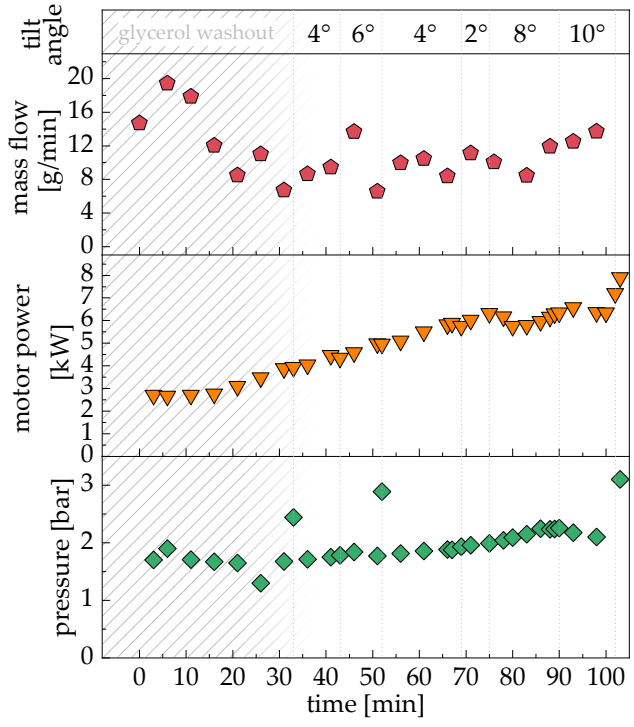


Figure 9. Different process parameters over the processing time during a continuous grinding experiment. Vertical guidelines indicate changes in the tilt angle.

Two pressure spikes were countered by tilting the mill to 4°, resulting in an increased mass flow rate. Over the runtime, further adjustments to the tilt angle were executed, based on the available process data. The continuously increasing power draw, which after 75 min had risen by 100% compared to the start of washout, required major adjustments to 8° and 10°, each time stabilizing the power draw briefly. This was interpreted as the opening of a blockage. Shortly thereafter, power consumption (and pressure) abruptly spiked above the motor's limit and the run was terminated. Crystallization of melt in the annular gap or at the mechanical seals could have led to such an increase in the power consumption, but the monitored temperatures were constantly above the melting temperature of xylitol. Upon disassembly of the mill, the rotor was visually inspected. Adhering melt at the inlet was discolored grey, while the melt at the outlet was still white. This was previously observed under packing conditions (compare Figure 6). The applicability of the tilting strategy during the run was confirmed to control grinding media packing.

4. Conclusions

Within this study, a continuous production of SCS from powdery raw material was demonstrated. The combination of extrusion and adapted wet milling successfully yielded a product containing large amounts of submicron particles from a single passage. A solution to the common issue of grinding media compression in annular gap mills was introduced. By inclining the mill, an operating point can be found, where the grinding media is equally distributed in an axial force balance. For Newtonian fluids, this strategy solves the usual trade-off between optimum stressing conditions, viscosity, productivity, and wear. In the case of an SCS suspension, the comminution progresses along the mill's axis, such that a viscosity gradient is formed by the growing interparticle interactions. An automated mechanism is needed to ensure a uniform grinding media distribution axially. Overall, the developed process is promising based on the results obtained from the prototype apparatus.

Author Contributions: Conceptualization, P.d.I. and M.T.; methodology, P.d.I. and M.T.; validation, P.d.I.; formal analysis, P.d.I. and J.B.; investigation, P.d.I., T.G. and J.B.; writing—original draft preparation, P.d.I.; writing—review and editing, J.B. and M.T.; visualization, P.d.I.; supervision, M.T. All authors have read and agreed to the published version of the manuscript.

Funding: This research received no external funding.

Data Availability Statement: The data presented in this study are available on request from the corresponding author.

Acknowledgments: The authors would like to thank Vanessa Düphans for providing 3D models of the individual screw elements.

Conflicts of Interest: Author Philip da Igreja was employed by the company INVITE GmbH. The remaining authors declare that the research was conducted in the absence of any commercial or financial relationships that could be construed as a potential conflict of interest.

References

1. Amidon, G.L.; Lennernäs, H.; Shah, V.P.; Crison, J.R. A theoretical basis for a biopharmaceutic drug classification: The correlation of in vitro drug product dissolution and in vivo bioavailability. *Pharm. Res.* **1995**, *12*, 413–420. [CrossRef] [PubMed]
2. Hagedorn, M.; Liebich, L.; Bögershausen, A.; Massing, U.; Hoffmann, S.; Mende, S.; Rischer, M. Rapid development of API nano-formulations from screening to production combining dual centrifugation and wet agitator bead milling. *Int. J. Pharm.* **2019**, *565*, 187–198. [CrossRef] [PubMed]
3. Thommes, M.; Ely, D.R.; Carvajal, M.T.; Pinal, R. Improvement of the dissolution rate of poorly soluble drugs by solid crystal suspensions. *Mol. Pharm.* **2011**, *8*, 727–735. [CrossRef] [PubMed]
4. Thommes, M.; Pinal, R.; Carvajal, M.T. Solid Formulations of Crystalline Compounds. Patent WO 2009/052391 Al, 23 April 2009.
5. Reitz, E. Extrudierte Feste Dispersionen zur Verbesserung der Lösungsgeschwindigkeit und Bioverfügbarkeit. Ph.D. Thesis, Heinrich-Heine-Universität, Düsseldorf, Germany, 2014.
6. Mühlenfeld, C. Herstellung Fester Dispersionen Durch Covermahlung. Ph.D. Thesis, Heinrich-Heine-Universität, Düsseldorf, Germany, 2013.

7. da Igreja, P.; Erve, A.; Thommes, M. Melt milling as manufacturing method for solid crystalline suspensions. *Eur. J. Pharm. Biopharm.* **2021**, *158*, 245–253. [CrossRef] [PubMed]
8. Da Igreja, P.; Klump, D.; Bartsch, J.; Thommes, M. Reduction of submicron particle agglomeration via melt foaming in solid crystalline suspension. *J. Dispers. Sci. Technol.* **2022**, *45*, 307–316. [CrossRef]
9. Domokos, A.; Nagy, B.; Szilágyi, B.; Marosi, G.; Nagy, Z.K. Integrated Continuous Pharmaceutical Technologies—A Review. *Org. Process Res. Dev.* **2021**, *25*, 721–739. [CrossRef]
10. Lee, S.L.; O'Connor, T.F.; Yang, X.; Cruz, C.N.; Chatterjee, S.; Madurawe, R.D.; Moore, C.M.V.; Yu, L.X.; Woodcock, J. Modernizing Pharmaceutical Manufacturing: From Batch to Continuous Production. *J. Pharm. Innov.* **2015**, *10*, 191–199. [CrossRef]
11. Hyer, A.; Gregory, D.; Kay, K.; Le, Q.; Turnage, J.; Gupton, F.; Ferri, J.K. Continuous Manufacturing of Active Pharmaceutical Ingredients: Current Trends and Perspectives. *Adv. Synth. Catal.* **2024**, *366*, 357–389. [CrossRef]
12. Junghanns, J.-U.A.H.; Müller, R.H. Nanocrystal technology, drug delivery and clinical applications. *Int. J. Nanomed.* **2008**, *3*, 295–309. [CrossRef]
13. Holland, S.; Knight, W.; Leonard, G. Wet Milling Process. U.S. Patent 2006/0214037 A1, 28 September 2006.
14. Monteiro, A.; Afolabi, A.; Bilgili, E. Continuous production of drug nanoparticle suspensions via wet stirred media milling: A fresh look at the Rehbinder effect. *Drug Dev. Ind. Pharm.* **2013**, *39*, 266–283. [CrossRef] [PubMed]
15. Merisko-Liversidge, E.M.; Liversidge, G.G. Drug nanoparticles: Formulating poorly water-soluble compounds. *Toxicol. Pathol.* **2008**, *36*, 43–48. [CrossRef] [PubMed]
16. Liversidge, G.G. Surface Modified Drug Nanoparticles. U.S. Patent 5145684, 8 September 1992.
17. Müller, R.H.; Jacobs, C.; Kayser, O. Nanosuspensions as particulate drug formulations in therapy. Rationale for development and what we can expect for the future. *Adv. Drug Deliv. Rev.* **2001**, *47*, 3–19. [CrossRef] [PubMed]
18. Müller, R.H. Pharmaceutical Nanosuspensions for Medicament Administration as System with Increased Saturation Solubility and Rate of Solution. U.S. Patent 5858410, 12 January 1999.
19. Kipp, J.E. Method for Preparing Submicron Particle Suspensions. U.S. Patent 6884436 B2, 26 April 2005.
20. Stehr, N. Residence time distributions in a stirred ball mill and their effect on comminution. *Chem. Eng. Process. Process Intensif.* **1984**, *18*, 73–83. [CrossRef]
21. Kwade, A.; Schwedes, J. Wet Grinding in Stirred Media Mills. In *Particle Breakage*; Elsevier: Amsterdam, The Netherlands, 2007; pp. 251–382. ISBN 9780444530806.
22. Schubert, K.; Bauckhage, K. *Handbuch der Mechanischen Verfahrenstechnik*; Wiley: Hoboken, NJ, USA, 2005.
23. Hennart, S.; van Hee, P.; Drouet, V.; Domingues, M.C.; Wildeboer, W.J.; Meesters, G. Characterization and modeling of a sub-micron milling process limited by agglomeration phenomena. *Chem. Eng. Sci.* **2012**, *71*, 484–495. [CrossRef]
24. Mavros, P. Technical note validity and limitations of the closed-vessel analytical solution to the axial dispersion model. *Miner. Eng.* **1992**, *5*, 1053–1060. [CrossRef]
25. Schons, D.; Kwade, A. Determination of the axial grinding media distribution in the IsaMill using radiometric densitometry. *Miner. Eng.* **2019**, *130*, 110–116. [CrossRef]
26. Stehr, N. Möglichkeiten zur Verhinderung der Mahlkörper-Verpressung in kontinuierlich betriebenen Rührwerksmühlen. *Chem. Ing. Tech.* **1989**, *61*, 422–423. [CrossRef]

Disclaimer/Publisher's Note: The statements, opinions and data contained in all publications are solely those of the individual author(s) and contributor(s) and not of MDPI and/or the editor(s). MDPI and/or the editor(s) disclaim responsibility for any injury to people or property resulting from any ideas, methods, instructions or products referred to in the content.